

Gautam Basu · Mark Allen · Deborah Willits
Mark Young · Trevor Douglas

Metal binding to cowpea chlorotic mottle virus using terbium(III) fluorescence

Received: 26 March 2003 / Accepted: 19 May 2003 / Published online: 9 July 2003
© SBIC 2003

Abstract Metals are thought to play a role in the structure of many viruses. The crystal structure of the $T=3$ icosahedral cowpea chlorotic mottle virus (CCMV) suggests the presence of 180 unique metal-binding sites in the assembled protein cage. Each of these sites is thought to involve the coordination of the metal by five amino acids contributed from two adjacent coat protein subunits. We have used fluorescence resonance energy transfer (FRET), from tryptophan residues proximal to the putative metal-binding sites, to probe Tb(III) binding to the virus. Binding of Tb(III) was investigated on the wild-type virus and a mutant where the RNA binding ability of the virus was removed. Tb(III) binding was observed both in the wild-type virus ($K_d = 19 \mu\text{M}$) and the mutant ($K_d = 17 \mu\text{M}$), as monitored by the increase in Tb(III) fluorescence (545 nm) and concomitant decrease in tryptophan fluorescence (342 nm). Competitive binding experiments showed Ca(II) to have about 100-fold less affinity for the binding sites ($K_d = 1.97 \text{ mM}$). This is the first direct evidence of metal binding to the putative metal-binding sites, originally suggested from the crystal structure of CCMV.

Keywords Cowpea chlorotic mottle virus · Fluorescence resonance energy transfer · Metal–RNA binding · Metal–virus binding · Terbium

Introduction

Metals often play an essential role in macromolecular protein assembly [1, 2, 3]. For example, viral capsids are typically assembled from a limited set of protein subunits that often involve metal coordination [4]. In addition, many virus particles can undergo dramatic structural transitions, often associated with processes of infection. The influenza virus, for example, undergoes dramatic structural transitions to release its nucleic acid into the cell [5]. A small spherical plant virus, cowpea chlorotic mottle virus (CCMV), has been a model system for understanding the chemical basis of virion assembly for the past 30 years [6, 7, 8]. The virion is comprised of 180 identical copies of a single coat-protein subunit which assemble into 28 nm $T=3$ icosahedral particles (Fig. 1) both in vivo and in vitro. The CCMV virion encapsulates an approximately 2.3 kb single-stranded RNA genome [9]. The RNA is predominantly associated with the protein shell through an electrostatic interaction with the basic N-terminus, composed of nine Arg and Lys residues, in each coat-protein subunit. In vitro, at neutral pH, the assembly of CCMV is dependent on the presence of divalent metal ions, such as Ca^{2+} [10, 11]. Putative metal-binding sites have been suggested by the CCMV crystal structure, but full occupancy of these sites was not observed due to the low pH conditions (pH 3.2) used for crystallization [12]. This illustrates that once the CCMV virion is assembled, the bound metal ions are labile and can be removed by substantially reducing the pH. In addition, metals can be removed from the virus at near neutral pH by chelating agents, without causing virion disassembly. The crystal structure suggests that the putative metal-binding sites are located at the 60 separate quasi-three-fold axes formed

M. Allen · T. Douglas (✉)
Department of Chemistry and Biochemistry,
Montana State University, Bozeman, MT 59717, USA:
E-mail: tdouglas@chemistry.montana.edu
Tel.: +1-406-9946566
Fax: +1-406-9945407

D. Willits · M. Young (✉)
Department of Plant Sciences,
Montana State University, Bozeman, MT 59717, USA
E-mail: myoung@montana.edu
Tel.: +1-406-9945158
Fax: +1-406-9947600

G. Basu
Department of Biophysics, Bose Institute,
700 054 Calcutta, India

Present address: G. Basu
Graduate School of Information Science,
Nara Institute of Science and Technology,
8916-5 Takayama, Ikoma, 630-0101 Nara, Japan

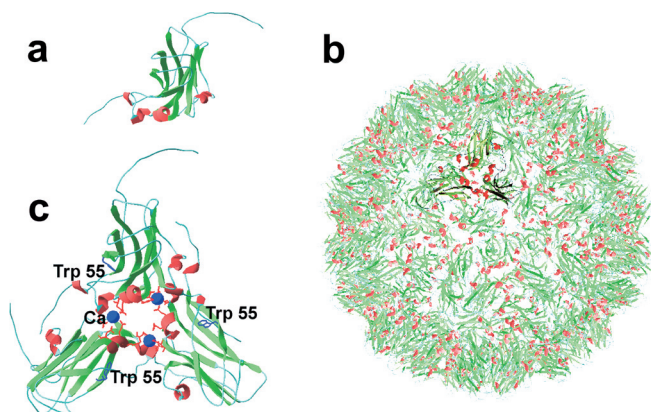


Fig. 1 Ribbon diagram of the $T=3$ icosahedral cowpea chlorotic mottle virus (CCMV; pdb 1cwp): (a) subunit showing α helices in red and β sheets in green; (b) the assembled 180 subunit virion with the asymmetric unit shown; (c) three subunits form the asymmetric unit with putative Ca(II) binding site (residues E81, E148, D153, Q85, and Q149 in red) coordinating the Ca ions (blue). The sidechain of Trp55 is shown in blue

at the interface between three coat-protein subunits (Fig. 1). There are three putative metal-binding sites at each of these axes, leading to 180 sites in the assembled $T=3$ virion. The coordination of the Ca^{2+} ion at these sites has been modeled and is thought to include the carboxylic oxygens of three acidic residues (E81, E148, and D153) and the carbonyl oxygens of two polar groups (Q85 and Q149) [12, 13]. Removal of metals from these sites, at near neutral pH, causes a structural transition, resulting in the swelling of the virion. Below pH 6.5, the suspected sidechains coordinating the metal ions are protonated. Under these conditions the virus is in its closed (unswollen) conformation, independent of the presence or absence of metal ions. The swelling structural transition is a result of expansion at the pseudo-three-fold axis centered around the putative metal-binding sites. However, there is little direct biochemical information regarding the metal binding at the putative metal-binding sites.

We have used fluorescence resonance energy transfer (FRET) to probe the metal-binding characteristics of CCMV with two different metal ions [Ca(II) and Tb(III)] that have physiological significance or spectroscopic advantages. Both wild-type virus and a genetically altered virus have been used. The genetically altered virus used in this study is not capable of packaging nucleic acid and has allowed us to directly compare metal binding to CCMV in the presence and absence of packaged viral RNA.

Materials and methods

CCMV virions used in binding studies

Two forms of CCMV virions were used in these experiments: the wild-type virus (wt CCMV) which contained the native viral RNA, and a mutant form of CCMV, devoid of the viral RNA [14]. The

wild type was purified to homogeneity from infected cowpea plants [11], while the mutant virus capsid was purified from a yeast heterologous expression system [14]. In this mutant, termed subE, eight basic N-terminal amino acids (K8, K20, K22, R11, R14, R15, R19, and R23) have been altered to the acidic glutamic acid (E) residue using QuikChange site-directed mutagenesis (Stratagene, La Jolla, Calif.). Immediately prior to fluorescence experiments, the virions were fractionated using size exclusion chromatography (Superose 6, Amersham Biosciences, Uppsala, Sweden; 50 mM MES, pH 6.5) to eliminate any aggregates or subunit disassembly products potentially present in the samples. Purified virions were analyzed by dynamic light scattering (ZetaPlus, Brookhaven Instruments), SDS-PAGE, and directly visualized using transmission electron microscopy (Leo 912 at 100 kV) of negatively stained samples (1% uranyl acetate). Protein concentration was determined by the absorbance at 280 nm ($\epsilon=24,075 \text{ M}^{-1} \text{ cm}^{-1}$) and confirmed using a biuret assay [15].

Fluorescence

All fluorescence experiments were performed on a SPEX Fluoromax2 or a Fluorolog spectrophotometer at 25 °C. Excitation and emission slit widths were set to 4 and 8 nm, respectively. The fluorescence spectrum of tryptophan in the native CCMV was measured ($\lambda_{\text{max}}=342 \text{ nm}$) following excitation at 295 nm. A stock solution (250 mM) of $\text{Tb}(\text{NO}_3)_3$ was prepared in pure water (18 M Ω resistivity) and diluted to give a working solution of 25 mM for Tb(III) binding studies. The concentrations of both solutions were independently measured by atomic emission inductively coupled plasma (AE ICP) measurements. Fluorescence was measured on solutions of virus (2.0 mL, 2 μM , 5 μM , or 7 μM subunit concentration) to which metal ion was added in 5–20 μL increments. The first 12 additions were 10 μL of metal solution (0.25 mM) and six subsequent additions were 5 μL of metal ion solution at 2.5 mM concentration. All fluorescence experiments were independently measured at least three times. FRET from tryptophan to bound Tb resulted in typical Tb(III) emission [16], where the 545 nm peak ($^5\text{D}_4 \rightarrow ^7\text{F}_5$) was monitored in the present study. The pH of the samples was buffered at 6.5 (50 mM MES, 50 mM NaCl).

Calculation of metal-binding isotherm and dissociation constants

In analyzing the data for Tb(III) binding to the CCMV protein cage, we have made the underlying assumption that all 180 sites are invariant, with identical affinities. Assuming an average of one binding site per subunit allows us to use a simple single-site model (Eq. 1) to analyze the data:

$$\phi_B = \frac{[\text{Tb(III)}]_F}{[\text{Tb(III)}]_F + K_d} \quad (1)$$

where ϕ_B is the fraction of CCMV bound to Tb(III), $[\text{Tb(III)}]_F$ is the free Tb(III) concentration, and K_d is the dissociation constant.

Fluorescence data were collected after addition of each aliquot of Tb(III) and fluorescence intensities monitored at 342 nm (tryptophan emission) and at 545 nm (Tb(III) emission). After baseline correction, the fluorescence spectra around the $^5\text{D}_4 \rightarrow ^7\text{F}_5$ peak (530–570 nm) were individually fit with a Gaussian function to find the maximum intensity. Values of ϕ_B were estimated independently for the 342 nm emission (decreasing intensity indicating increased FRET) and 545 nm emission (increasing intensity indicating increased FRET) data. For the 545 nm data we used $\phi_B = I_{545}/I_{545}^{\text{max}}$ while for the 342 nm data $\phi_B = (I_{342}^0 - I_{342})/(I_{342}^0 - I_{342}^{\text{min}})$ was used, where I_{342}^0 represents the initial intensity at 342 nm while I_{342}^{min} and I_{545}^{max} represent the limiting intensities (at high Tb(III) concentration). The limiting intensities were estimated by fitting the raw data (fluorescence intensity versus total Tb(III) concentration) to a rectangular hyperbola (similar to Eq. 1). Values of $[\text{Tb(III)}]_F$

were estimated from the total Tb(III) concentration, $[Tb(III)]_T$, and total CCMV concentration, $[CCMV]_T$, as: $[Tb(III)]_F = [Tb(III)]_T - \phi_B [CCMV]_T$.

Competitive binding experiments were performed to assess the relative affinities of a second ion, e.g. Ca(II), to the Tb(III) binding site. The apparent relative binding affinity of the second ion X, K_{app} , is related to the decrease in Tb(III) fluorescence, I_{545} , as a function of total concentration of X as:

$$I_{545} = \frac{I_{545}^{max} K_{app}}{K_{app} + [X]_T} + I_{545}^{lim} \quad (2)$$

where $[X]_T$ is the total concentration of X and I_{545}^{lim} is the limiting value of I_{545} at high $[X]_T$. The dissociation constant for X, K_d^X was then obtained from [17]:

$$K_d^X = \frac{K_{app}}{1 + \frac{[Tb(III)]_T}{K_d^{Tb(III)}}} \quad (3)$$

Results

In the assembled virus particle, each subunit has an endogenous tryptophan residue (W55) located approximately 1.5 nm from the putative metal-binding site (Fig. 1C). This provides an ideal geometry for using FRET to probe the metal binding at this site. Upon excitation of the tryptophan at 295 nm, FRET to the fluorescent lanthanide ion, Tb(III), was observed when it occupied the metal-binding site. Thus, by monitoring the increase in Tb(III) fluorescence, and concomitant loss of tryptophan fluorescence, as a function of added Tb(III), we have probed the metal-binding characteristics of this site. The resulting hyperbolic binding isotherms have been modeled to yield apparent dissociation constants for Tb(III) binding to the putative binding sites.

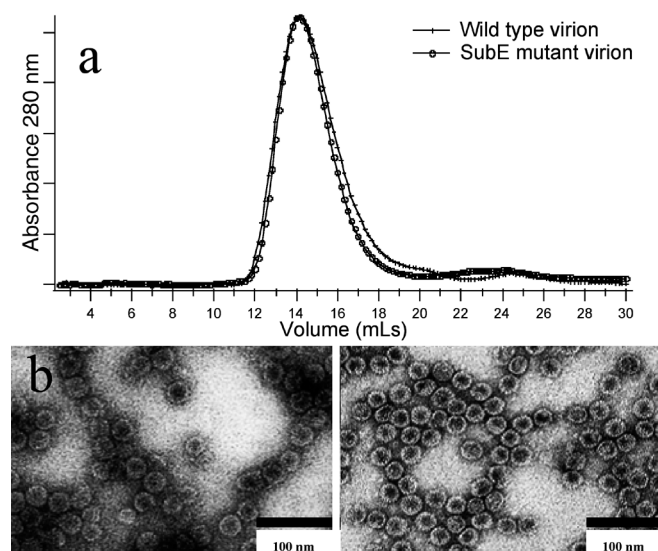


Fig. 2 Characterization of the assembled CCMV virion: (a) size exclusion chromatography of wild-type and subE mutant virions; (b) transmission electron micrograph of the wild-type (left) and subE (right) virions, negatively stained with uranyl acetate (scalebar is 100 nm)

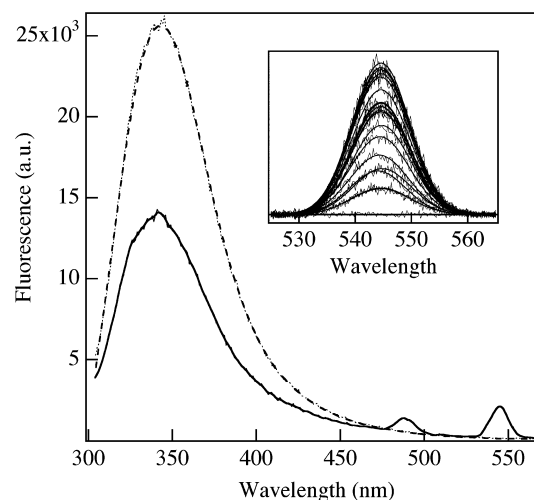


Fig. 3 Fluorescence spectra of wild-type CCMV, in the absence (broken line) and in the presence of Tb(III) (solid line). The growth of the Tb(III) peak at 545 nm as a function of increasing Tb(III) is illustrated in the inset. The corresponding binding isotherm is shown in Fig. 4

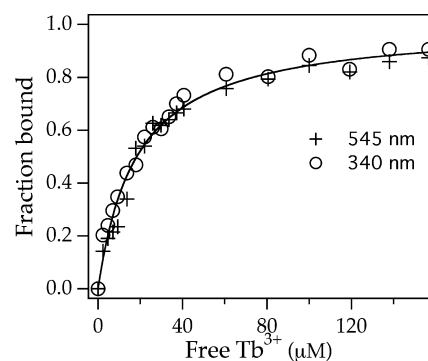


Fig. 4 Tb(III) binding isotherm for wild-type CCMV (5 μ M subunit concentration; pH 6.5 and 25 $^{\circ}$ C). Following excitation at 295 nm, the binding isotherm was constructed by monitoring the increase in fluorescence emission at 545 nm and concomitant decrease at 342 nm. A global fit of both data sets to Eq. 1 yielded $K_d = 19 \mu$ M

Initially we examined Tb(III) binding to highly purified wild-type CCMV. The purity of the protein component was assessed by SDS-PAGE and the RNA component by the A_{260}/A_{280} ratio of the absorbance, which was found to be 1.7. As expected, the purified virus was assembled into 28-nm diameter $T=3$ icosahedral particles, as determined by size exclusion chromatography, electron microscopy (Fig. 2), and dynamic light scattering.

Tb(III) binding to CCMV was measured at pH 6.5. Fluorescence of the endogenous tryptophan was monitored at 342 nm after excitation at 295 nm. On addition of Tb(III) to CCMV there was a decrease in the emission at 342 nm with increasing Tb (Fig. 3). The decrease in emission at 342 nm eventually reached a plateau, suggesting saturation of the binding site (Fig. 4). This decrease in emission at 342 nm was accompanied by a

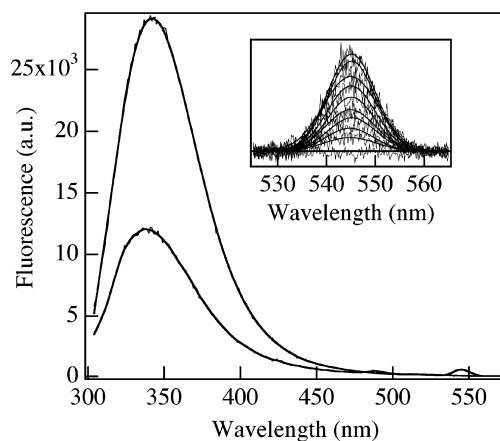


Fig. 5 Fluorescence spectra of the SubE mutant of CCMV, in the absence (*broken line*) and in the presence of Tb(III) (*solid line*). The growth of the Tb(III) peak at 545 nm as a function of increasing Tb(III) is illustrated in the *inset*. The corresponding binding isotherm is shown in Fig. 6

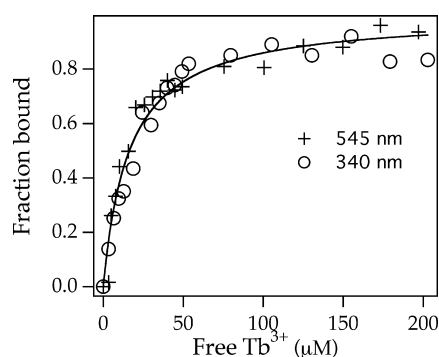


Fig. 6 Tb(III) binding isotherm for subE mutant of CCMV (5 μM subunit concentration; pH 6.5 and 25 $^{\circ}\text{C}$). Following excitation at 295 nm, the binding isotherm was constructed by monitoring the increase in fluorescence emission at 545 nm and concomitant decrease at 342 nm. A global fit of both data sets to Eq. 1 yielded $K_d = 17 \mu\text{M}$

concomitant increase in the emission at 545 nm (Fig. 3), which also saturated at the same Tb(III) concentrations. The binding isotherms depicting the fraction saturation as a function of free Tb(III) is shown for both the loss of tryptophan fluorescence and increase in Tb(III) fluorescence in Fig. 4. A global fit to fraction saturation data (both 545 nm and 342 nm data) to Eq. 1 yielded $K_d = 19 \mu\text{M}$ for wild-type CCMV. These data support the model that the increase in Tb fluorescence can be associated with FRET from tryptophan.

To examine if the presence of viral RNA affects metal binding to the coat protein, we examined the Tb(III) binding in the absence of any viral nucleic acid. This was accomplished by taking advantage of the subE mutant in which eight of the basic residues at the N-terminus were exchanged for the acidic residue glutamic acid. The purity of the protein component was assessed by SDS-PAGE. This mutant assembled into 28-nm diam-

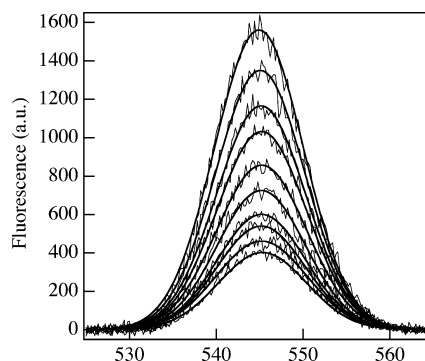


Fig. 7 The disappearance of Tb(III) emission (545 nm band) in wild-type CCMV ([subunit]=3 μM ; [Tb(III)]=38.1 μM) as a function of increasing Ca(II) concentration. The corresponding competitive binding analysis is shown in Fig. 8

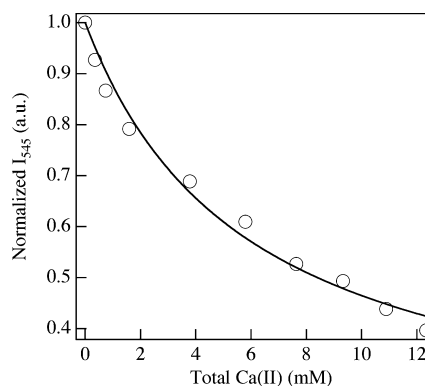


Fig. 8 Normalized (to volume changes) intensity values of Tb(III) emission (545 nm) in wild-type CCMV ([subunit]=3 μM ; [Tb(III)]=38.1 μM) as a function of increasing Ca(II) concentration. A fit of the data to Eq. 2 yielded $K_{app} = 5.9 \text{ mM}$, resulting in a K_d^X (Eq. 3) value of 1.97 mM

eter $T=3$ icosahedral particles indistinguishable from wild-type particles, as determined by size exclusion chromatography, electron microscopy, and dynamic light scattering both prior to and following metal binding studies (Fig. 2). In contrast to wild-type virus particles, the subE protein cage was determined to be empty of RNA by electron microscopy and UV spectroscopy, in which the A_{260}/A_{280} ratio was determined to be 0.8.

The purified subE virions were used to examine Tb(III) binding in the absence of any RNA. Tb(III) binding to subE was measured at pH 6.5, and fluorescence of the endogenous tryptophan was monitored at 342 nm after excitation at 295 nm. Similar to the wild-type virus, on addition of Tb(III) to the subE mutant there was a decrease in the emission at 342 nm with increasing added Tb(III) (Fig. 5). This decrease in emission at 342 nm was accompanied by an identical relative concomitant increase in the emission at 545 nm associated with FRET. Both the decrease in tryptophan emission at 342 nm and the increase in Tb(III) emission at 545 nm reached a plateau at similar Tb(III) concentrations, suggesting saturation of the binding sites

(Fig. 6). The binding isotherms depicting the fraction saturation as a function of free Tb(III) is shown for both the loss of tryptophan fluorescence and increase in Tb(III) fluorescence (Fig. 6). From a global fit of these data (to Eq. 1), the estimated dissociation constant for Tb binding to 180 quasi-equivalent binding sites in subE is $K_d = 17 \mu\text{M}$. Like wild-type CCMV, the subE mutant has a similar affinity for Tb(III), suggesting that the RNA does not play a significant role in Tb(III) binding. The subE mutant has allowed us to quantify metal binding to the assembled viral protein cage in the absence of any nucleic acid.

To investigate the binding of the biologically relevant Ca(II) to CCMV, we used a competitive binding assay between Tb(III) and Ca(II). CCMV (wild type) saturated with Tb(III) was exposed to increasing amounts of Ca(II) and both tryptophan and Tb(III) fluorescence were monitored at 342 nm and 545 nm, respectively. With increasing Ca(II) there was an associated increase in the tryptophan fluorescence (not shown) and a concomitant decrease in the Tb(III) fluorescence at 545 nm (Fig. 7). These data were fit to Eq. 2 and yielded a dissociation constant, $K_d^X = 1.97 \text{ mM}$, for Ca(II) binding to CCMV (Fig. 8; Eqs. 2 and 3). This indicates that the Ca(II) affinity is approximately 100-fold lower than that observed for Tb(III) binding.

Discussion

In this study we have investigated the metal–protein interactions in the assembled plant virus CCMV. This is the first quantitative analysis of metal binding to a virus. Using the fluorescent lanthanide ion Tb(III), a well-established and effective mimic for Ca(II), we have exploited FRET to probe the metal interactions with the virus in the presence and absence of nucleic acid. Experiments with wild-type virus suggest the presence of a metal-binding site in close proximity to a tryptophan residue. This corresponds well with the putative metal-binding sites suggested by the crystal structure, originating from a coordination of the metal by five amino acid residues contributed from two adjacent subunits. In the assembled virus particle there are 180 of these sites. Owing to the $T=3$ icosahedral symmetry of the virus, these sites are not strictly equivalent, but are quasi-equivalent and for our analysis we have assumed that they are functionally identical.

Genetic engineering has allowed us to investigate the specific contribution of the virion protein shell to metal binding. In the subE mutant we removed the ability of the virion to bind nucleic acid, which allowed us to study the metal binding to the viral capsid in isolation. We found that metal binding to CCMV, with a $K_d \approx 20 \mu\text{M}$, was independent of the presence of the viral nucleic acid. At first glance it might seem surprising that the polyanionic RNA contributes so little to the overall metal binding. However, consideration of the nine basic

residues on each coat protein N-terminus, and 13 basic residues identified as nucleic acid binding sites from the crystal structure, suggests that there are few anionic sites remaining for metal binding to RNA. The RNA could also play a role in virion structural transitions (swelling), which are known to be metal ion dependent [12, 18]. Our data suggest that the RNA does not play a critical role and that the protein–metal ion interactions predominate. This is also consistent with our observations that RNA-free subE virions undergo swelling.

The 100-fold difference in binding affinity between Tb(III) and Ca(II) is consistent with their difference in charge. Other studies have shown similar range of affinities for these two metal ions. From a biological viewpoint, the Ca(II) binding appears weak, which may have important implications in virus replication. The biological role of metals in virus particle structure, assembly, and replication are not well understood. Many viruses are known to bind metals and the existence of the coordinated metal-binding sites suggests that they have a role in virus infection and replication [19]. Future studies should focus on the direct in vivo role of physiologically relevant metals (Ca, Mg) on the CCMV replication cycle.

Acknowledgements This work was supported in part by the National Institutes of Health (ROI GM61340) and the Office of Naval Research.

References

1. Durham AC, Hendry DA (1977) *Virology* 77:510–519
2. Hull R (1977) *Virology* 79:58–66
3. Durham AC, Bancroft JB (1979) *Virology* 93:246–252
4. Chiu W, Burnett R, Garcea R (eds) (1997) *Structural biology of viruses*. Oxford University Press, Oxford
5. Skehel JJ, Wiley DC (2000) *Annu Rev Biochem* 69:531–569
6. Bancroft JB, Hiebert E, Rees MW, Markham R (1968) *Virology* 34:224–239.
7. Fox JM, Johnson JE, Young MJ (1994) *Sem Virol* 5:51–60
8. Zlotnick A, Aldrich R, Johnson JM, Ceres P, Young MJ (2000) *Virology* 277:450–456
9. Ahlquist P (1999) In: Granoff A, Webster RG (eds) *Encyclopedia of virology*. Academic Press, New York, pp 198–204
10. Bancroft JB, Hiebert E (1967) *Virology* 32:354–356
11. Zhao X, Fox JM, Olson NH, Baker TS, Young MJ (1995) *Virology* 207:486–494
12. Speir JA, Munshi S, Wang G, Baker TS, Johnson JE (1995) *Structure* 3:63–78
13. Johnson JE, Speir JA (1997) *J Mol Biol* 269:665–675
14. Douglas T, Strable E, Willits D, Aitouchen A, Libera M, Young M (2002) *Adv Mater* 14:415–418
15. Sambrook J, Fritsch EF, Maniatis T (1989) *Molecular cloning: a laboratory manual*. Cold Spring Harbor Laboratory Press, Cold Spring Harbor, NY
16. Horrocks WD, Sudnick D (1981) *Acc Chem Res* 14:384–392
17. Cheng Y, Prusoff WH (1973) *Biochem Pharmacol* 22:3099–3108
18. Incardona NL, Flanagan JB, McKee S (1973) *Virology* 53:204–214
19. Liddington RC, Yan Y, Moulai J, Sahli R, Benjamin TL, Harrison SC (1991) *Nature* 354:278–284